Epitaxial Growth of Highly Conductive α-Ga_2O_3 by Suboxide Molecular-Beam Epitaxy

Julianne Chen[1], Jacob Steele[2], and Darrell G. Schlom[2, 3, 4]

[1]*Department of Materials Science and Engineering, The Pennsylvania State University, State College, 16802, Pennsylvania, USA*

[2]*Department of Materials Science and Engineering, Cornell University, Ithaca, 14853, New York, USA*

[3]*Kavli Institute at Cornell for Nanoscale Science, Ithaca, 14853, New York, USA*

[4]*Leibniz-Institut für Kristallzüchtung, Max-Born-Str. 2, 12489 Berlin, Germany*

August 18, 2024

Abstract

Growth of alpha Ga_2O_3 on flat m-plane sapphire (Al_2O_3) substrates was achieved through a thin, high temperature alpha Ga_2O_3 buffer with 8% aluminum and growth conditions such as 480C film growth temperature and high ozone pressure of 5×10^{-6} torr. Record breaking results such as symmetrical rocking curve FWHM (0.167°), resistivity (1.67×10^{-3} Ωcm), mobility (81.7 $cm^2V^{-1}s^{-1}$), and dislocation density (2.48×10^{8} cm^{-2}) were achieved.

I. Introduction

The Baliga figure of merit (BFOM) is a metric for semiconductors which correlates device power dissipation to intrinsic material properties such as mobility or critical electric field.[1] Ultrawide bandgap semiconductors such as Ga_2O_3 or diamond have been researched as their higher BFOM values allow for more efficient high voltage devices.

There are many different phases of Ga_2O_3 that have been studied, with the most thermodynamically stable being the β phase, but the metastable α-Ga_2O_3 phase has garnered interest for its bandgap of 5.3 eV that can be extended to 8.6 eV by alloying with Al_2O_3.[2]

Molecular beam epitaxy (MBE) is a thin film growth technique which heats metal sources in an ultra-high vacuum which allows for molecules to be deposited on a substrate atomic layer by layer. Growth of α-Ga_2O_3 with conventional MBE requires a two-step process with the gallium reacting with background ozone to form an intermediate being the rate-limiting step. Suboxide MBE (*S*-MBE) supplies oxide intermediates instead of metal sources, skipping the rate-limiting step of materials such as α-Ga_2O_3.

II. Methods

X-ray diffraction (XRD) and X-ray reflectivity (XRR) measurements were performed using a PANalytical Empyrean system. Surface topography was investigated with atomic force microscopy (AFM) using an Asylum Research Cypher Environmental AFM. Growth of α-Ga_2O_3 was conducted via *S*-MBE with a Ga_2O and SiO_2 molecular beam.

10x10 mm^2 m-plane sapphire (Al_2O_3) substrates were used. Indium metal contacts were soldered onto the corners for Hall measurements.

III. Results & Discussion

M-plane sapphire substrates with nanometer tall steps grew films with respectable electrical properties. When using flat m-plane sapphire substrates, streaks of *β*-Ga_2O_3 or cracks formed, as shown in the

AFM below, which demonstrated directional conductivity along the steaks. Stepped substrates are not able to be effectively produced, so flat substrates must be used.

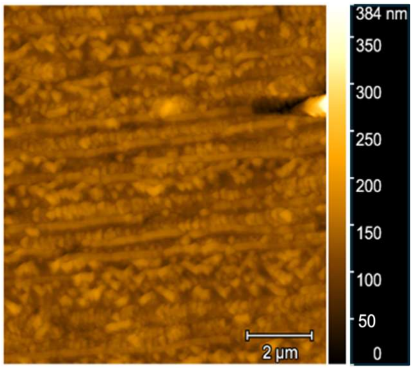

Figure 1: *Film growth on flat substrates, RMS of 24.5 nm, 436 nm thick sample*

Adding a buffer with low amounts of aluminum would reduce the 4% lattice mismatch between pure Al_2O_3 and α-Ga_2O_3 and not only prevent cracks from forming but promote α-Ga_2O_3 growth as α-Al_2O_3 and α-Ga_2O_3 are isostructural. The high temperature would allow the buffer to survive relaxation and allow the film to be strained to the buffer, preventing dislocations in the film that would form during the relaxation process. The buffer is thin, around 35 nm, to reduce the amount of growth time in a high temperature where β-Ga_2O_3 is more likely to form.

Films with a α-$(Al,Ga)_2O_3$ buffer, α-Ga_2O_3 buffer with no aluminum, and no buffer were grown at the same conditions.

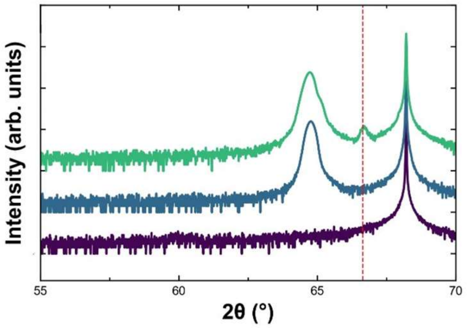

Figure 2: S1 has no buffer, S2 has a α-Ga_2O_3 buffer, and S3 has a α-$(Al,Ga)_2O_3$ buffer

α-Ga_2O_3 did not grow on the flat substrate without a buffer. Adding aluminum in the buffer increased mobility and lowered resistance. A hybrid peak, a peak created through interactions with the film and substrate which is associated with high order, was present in the film with aluminum in the buffer.

Property	α-Ga_2O_3	α-$(Al,Ga)_2O_3$
ρ	$64.2\ \Omega/\square$	$49\ \Omega/\square$
μ	$61.6\ cm^2/(V\cdot s)$	$78.8\ cm^2/(V\cdot s)$
FWHM	0.283°	0.167°

Table 1: *Properties of different buffer compositions*

Film growth temperature and ozone growth pressure were varied to optimize flat substrate films for conductivity. High pressures and low film temperatures resulted in a lower resistivity and FWHM than stepped substrates.

Property	Stepped	Flat
ρ	$7.4\times10^{-3}\ \Omega/\square$	$1.9\times10^{-3}\ \Omega/\square$
FWHM	0.352°	0.167°

Table 2: *ρ and FWHM of flat and stepped substrates*

The source temperature of SiO_2 was varied to control the carrier concentration. With decreased carriers, ionization scattering limits mobilities. However, the measurable points with our current contacts seem to indicate the typical mobility curve has been increased and shifted to the left. The high mobilities could be attributed to the high structural quality of our films, although better contacts would be needed to confirm our suspicions. Our films have exceeded the current literature records.

Parameter	Records	AlGa722	AlGa726
FWHM	0.27 [3]	0.167	0.185
R ($\Omega/\square$)	7.4×10^{-2} [4]	2.01×10^{-3}	1.67×10^{-3}
μ ($cm^2/V\cdot s$)	65 [5]	78.8	81.7
Dislocations (cm^{-2})	10^{11}-10^{12} [7, 8]	3.72×10^{8} [6]	2.48×10^{8}

Table 3: *Records versus our best films' properties*

IV. References

[1] B.J. Baliga, *Fundamentals of Power Semiconductor Devices*, 2nd ed. (Springer, 2019).

[2] R. Jinno, C.S. Chang, T. Onuma, Y. Cho, S.-T. Ho, D. Rowe, M.C. Cao, K. Lee, V. Protasenko, D.G. Schlom, D.A. Muller, H.G. Xing, and D. Jena, "Crystal orientation dictated epitaxy of ultrawide-bandgap 5.4- to 8.6-eV α-$(AlGa)_2O_3$ on m-plane sapphire," Sci. Adv. 7(2), eabd5891 (2021).

[3] M. Lee et al., Materials Science in Semiconductor Processing, vol. 123, no. 123, pp. 105565–105565, Mar. 2021, doi: https://doi.org/10.1016/j.mssp.2020.105565.

[4] S. Vogt et al., Physica Status Solidi, vol. 220, no. 3, Jan. 2023, doi: https://doi.org/10.1002/pssa.202200721.

[5] Akaiwa et al., Physica Status Solidi, vol. 217, no. 3, Jan. 2020, doi: https://doi.org/10.1002/pssa.201900632.

[6] J. E. Ayers, *Journal of Crystal Growth*, vol. 135, no. 1–2, pp. 71–77, Jan. 1994, doi: https://doi.org/10.1016/0022-0248(94)90727-7.

[7] K. Kaneko *et al*, *Japanese Journal of Applied Physics*, vol. 51, no. 2R, pp. 020201–020201, Jan. 2012, doi: https://doi.org/10.1143/jjap.51.020201.

[8] T. C. Ma *et al.*, *Applied Physics Letters*, vol. 115, no. 18, Oct. 2019, doi: https://doi.org/10.1063/1.5120554.

V. Supplementary Figures

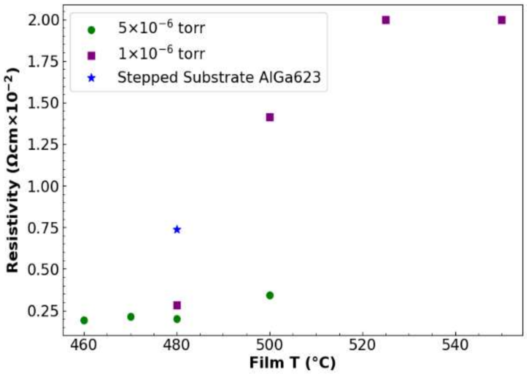

Figure 3: *film T and P_{O3} versus ρ*

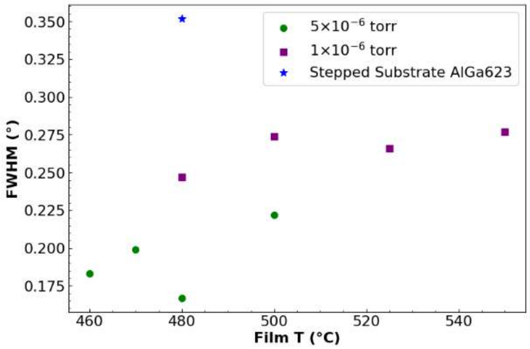

Figure 4: *film T and P_{O3} versus FWHM*

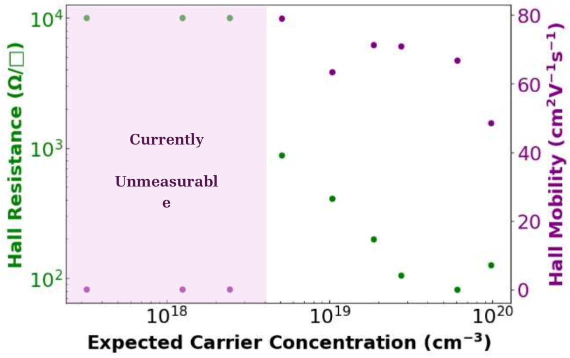

Figure 5: *Changing SiO_2 versus R and μ*

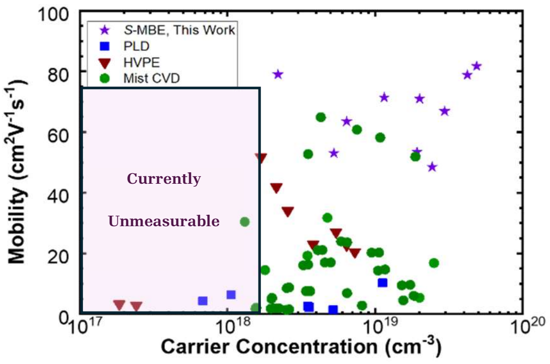

Figure 6: *Our work versus current literature μ*